Unsupervised Texture Segmentation Using Multiresolution Analysis for Feature Extraction

Kun Wardana Abyoto*, Sri Jatno Wirdjosoedirdjo**, and Tadashi Watanabe***

Abstract

The main difficulty of traditional texture segmentation is the lack of adequate tools to characterize different scales of textures effectively. Recent developments in multiresolution analysis such as wavelet transforms help to overcome this difficulty. This paper presents an approach of multiresolution analysis as textural feature extraction tool for segmenting remotely sensed image. The two-dimensional wavelet transform is used to decompose the input image into a multiresolution framework. The textural features derived from the statistical parameters are then extracted from each resolution of decomposed images. These features are used for the input of the clustering process. The procedure results in a segmented image whose regions are distinct from one another with respect to texture characteristic content. An artificial image made from Brodatz-like microtextures is selected to test the capability of the technique. Implementation to SPOT satellite image is also demonstrated. Experiments indicate that this method can be applied with promising results.

1. Introduction

Texture segmentation is an essential component of many image processing, computer graphic and computer vision techniques. The ability to discriminate textures is generally dependent of scale, rotation, and changes in illumination. Whenever a machine vision system is expected to perform the same texture discrimination task, it has to solve the problem of segmenting the image into uniformly textured regions, recognizing similar textures even if they are differently shaded or rotated. Texture is characterized not only by the gray value at a given pixel, but also by the gray value "pattern" in a neighborhood surrounding the pixel. Much research work has been done on texture analysis, classification, and segmentation for the last three decades. Despite the effort, texture analysis is still considered an interesting but difficult problem in image processing. Many methods share one common weakness; that is, they primarily focus on the coupling between image pixels on a single scale [1], [2], [14]. One difficulty of traditional texture analysis is the lack of an adequate tool that characterizes different scales of textures effectively. Recent developments in spatial/frequency analysis such as the Gabor transform, and wavelet transform provide good multiresolution analytical tools and should help to overcome this difficulty [6], [8], [9], [11].

A large class of natural textures can be detected by highly concentrated spatial

* Strategic Development Division, PT. Indosat, Indonesia
** Department of Physics, Bandung Institute of Technology, Indonesia
*** Department of Information Systems, Tokyo University of Information Sciences, Japan

1998年4月16日受理

frequencies and orientations. Recent study of the human vision system indicates that the spatial/frequency representation [8], which preserves both global and local information, is adequate for characterizing texture properties. This observation has motivated researchers to develop mutiresolution texture models [4], [6], [11], [15]. A new spatial/scale analysis known as wavelet theory has been under intensive study during the last ten years [8], [9]. More recently, the wavelet basis function has been generalized, to include a library of modulated waveform orthonormal basis called wavelet packets. The wavelet and wavelet packet transform can be implemented efficiently with pyramid- and tree-structured algorithms.

In this research, we apply tree-structured algorithm of multiresolution wavelet transform to texture segmentation application. The textural features are extracted using statistic parameters from the multiresolution framework. The fuzzy c-means method is used for the clustering process of these textural features. This process will result in a segmented image whose regions are distinct from one another with respect to texture characteristic content. A special synthetic image generated by combining four Brodatz-like microtextures is selected to test the capability of the technique. Then, an implementation to SPOT satellite image is illustrated.

This paper is organized as follows. Review of the multiresolution analysis based on wavelet transform is described in Section 2. In Section 3, we briefly discuss the theory of fuzzy c-means clustering. Section 4 shows the proposed procedure for texture segmentation using multiresolution analysis. Experimental results and discussion are presented in Section 5. Concluding remarks are given in Section 6.

2. Multiresolution Analysis Based on Wavelet Transform

The multiresolution wavelet transform decomposes a signal into the coarser resolution representation which consists of the low frequency approximation information and the high frequency detail information. During the decomposition, the resolution decreases exponentially at the base of 2. Let the convolution of two energy finite functions $f(x,y) \in L^2(R)$ and $g(x,y) \in L^2(R)$be

$$(fxg)(x,y) = \int_{-\infty}^{+\infty}\int_{-\infty}^{+\infty} f(u,v)g(x-u,y-v)du\ dv \tag{1}$$

The approximation of a two-dimension finite-energy function f(x,y) at resolution 2^j, where integer j is a decomposition level, can be characterized by the coefficient calculated by the following convolution:

$$A_{2^j}f = ((f(x,y) \times \phi_{2^j}(-x)\ \phi_{2^j}(-y))(2^{-j}n, 2^{-j}m)_{(n,m)\in Z^2} \tag{2}$$

where m, n are integers, $\phi(x)$ is a one-dimension scaling function, and $\phi_{2^j}(x) = 2^j\phi(2^jx)$. In general, the $\phi(x)$ is a smooth function whose Fourier transform is concentrated in low

frequencies. The difference between approximation information at two consecutive resolutions $2^j$and 2^{j-1}, which are characterized by $A_{2^j}f$ and $A_{2^{j-1}}f$, respectively, can be captured by the detail coefficients computed by the following convolutions:

$$D^1_{2^{j-1}}f = ((f(x,y) \times \phi_{2^{j-1}}(-x)\,\psi_{2^{j-1}}(-y))(2^{-(j-1)}n, 2^{-(j-1)}m)_{(n,m)\in Z^2} \quad (3)$$

$$D^2_{2^{j-1}}f = ((f(x,y) \times \psi_{2^{j-1}}(-x)\,\phi_{2^{j-1}}(-y))(2^{-(j-1)}n, 2^{-(j-1)}m)_{(n,m)\in Z^2} \quad (4)$$

$$D^3_{2^{j-1}}f = ((f(x,y) \times \psi_{2^{j-1}}(-x)\,\psi_{2^{j-1}}(-y))(2^{-(j-1)}n, 2^{-(j-1)}m)_{(n,m)\in Z^2} \quad (5)$$

where $\psi(x)$ is one-dimensional wavelet function and $\psi_{2^j}(x)= 2^j\psi(2^jx)$. The wavelet function $\psi(x)$ is a band-pass filter. $A_{2^j}f$ can be perfectly reconstructed from $A_{2^{j-1}}f$, $D^1_{2^{j-1}}f$, $D^2_{2^{j-1}}f$ and $D^3_{2^{j-1}}f$.

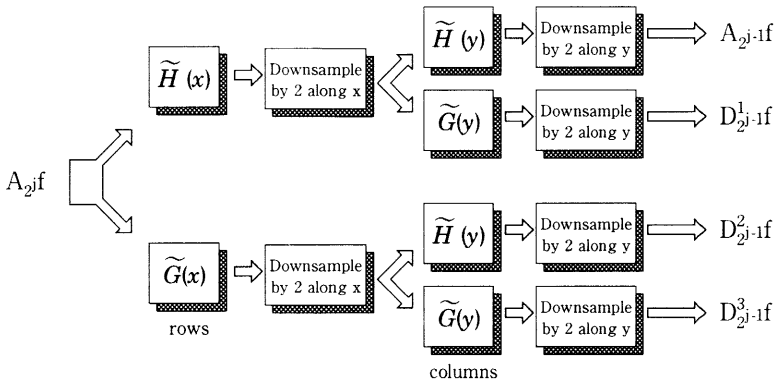

Figure 1. The docomposition of an image $A_{2^j}f$ into $A_{2^{j-1}}f$, $D^1_{2^{j-1}}f$, $D^2_{2^{j-1}}f$ and $D^3_{2^{j-1}}f$.

The approximation and detail coefficients can be calculated with a pyramid algorithm based on convolutions with two one-dimensional parameter filters. Figure 1 shows the decomposition of $A_{2^j}f$ into $A_{2^{j-1}}f$, $D^1_{2^{j-1}}f$, $D^2_{2^{j-1}}f$ and $D^3_{2^{j-1}}f$. $\widetilde{H}$ and $\widetilde{G}$ in figure 1 are one-dimension low-pass and one-dimension high-pass filters, respectively. The impulse response of filter $\widetilde{H}$ is given by $\widetilde{h}(n) = h(-n)$. The notation h(n) used in this paper is illustrated in table 1 (the 16-tap Daubechies wavelet). The impulse response of filter $\widetilde{G}$ is $\widetilde{g}(n) = g(-n)$, where $g(n) = (-1)^{1-n}h(1-n)$. As figure 1 shows, this algorithm first convolutes the rows of image $A_{2^j}f$ with the one-dimensional filter, retains every other column, convolutes the columns of the resulting signals with another one-dimensional filter and retains every other row. The pyramid decomposition can be continuously applied to the approximation image until the desired coarser resolution 2^{-J} (J>0) is reached.

Position	Value	Position	Value
h_0	0.054416	h_8	-0.017369
h_1	0.312872	h_9	-0.044088
h_2	0.675631	h_{10}	0.013981
h_3	0.585355	h_{11}	0.008746
h_4	-0.015829	h_{12}	-0.004870
h_5	-0.284016	h_{13}	-0.000392
h_6	0.000474	h_{14}	0.000675
h_7	0.128747	h_{15}	-0.000117

Table 1. Coefficients of h(n) used to generate 16-tap Daubechies wavelet.

We consider the original discrete image as A_1f which is measured at resolution 1. Thus, an original image A_1f is completely represented by one approximation image at resolution 2^{-J} and 3J detail images.

$$(A_{2^{-J}}f, (D^1_{2^j}f)_{-J\le j\le -1}, (D^2_{2^j}f)_{-J\le j\le -1}, (D^3_{2^j}f)_{-J\le j\le -1}) \tag{6}$$

Decomposition of the frequency support of the image $A_{2^{j+1}}f$ into $A_{2^j}f$ and the detail images $D^k_{2^j}f$ is illustrated in figure 2(a). The approximation image and detail images derived from decomposition are usually organized as shown in figure 2(b). No extra data are produced in the decomposition procedures because of the orthogonality of the wavelet representation [8]. The wavelet decomposition can be interpreted as a signal decomposition in a set of independent, spatially-oriented frequency channels. The image $A_{2^j}f$ corresponds to the lowest frequencies, $D^1_{2^j}f$ gives the vertical high frequencies (horizontal edges), $D^2_{2^j}f$ gives the horizontal high frequencies (vertical edges), and $D^3_{2^j}f$ gives the high frequencies in both directions (diagonal).

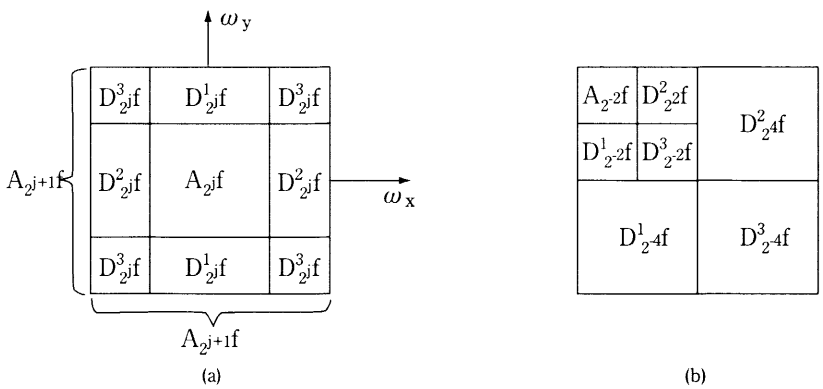

Figure 2. (a) Decomposition of the frequency support of the image $A_{2^{j+1}}f$ into $A_{2^j}f$ and the detail images $D^k_{2^j}f$. (b) Disposition of the $D^k_{2^j}f$ and $A_{2^{-j}}f$ images in the image wavelet representation.

The wavelet function $\psi_{2j}(x)$ has various resolution cell shapes in the spatial-frequency domain. When the decomposition level j decreases, the resolution decreases in the spatial domain and increases in the frequency domain. This variation of wavelet resolution enables the wavelet transform to zoom into the irregularities of the signal and characterize them locally.

Usually the image decomposition scheme is performed recursively to the low frequency channel $A_{2j}f$. However, since the most significant information of a texture often appears in the middle frequency channels, further decomposition just in the lower frequency region, such as the conventional wavelet transform does, may not help much for the purpose of segmentation.

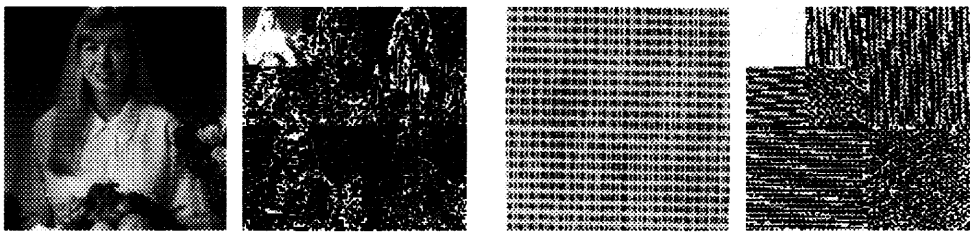

(a) (b)

Figure 3. Pyramid-structured wavelet transforms. (a) "Lady" image (b) "Texture" image

This concept can be illustrated in figure 3 where the pyramid-structured wavelet transform is applied to two different kinds of images. We use the lady image as a representative for an ordinary image. The image and its pyramid-structured wavelet transform are shown in figure 3(a). For comparison, we use the texture image shown with its pyramid-structured wavelet transform in figure 3(b). By examining the wavelet-transformed image in figure 3(a), we recognize the lady image clearly from its low frequency channel (the upper left corner). In contrast, we are not able to recognize a similar texture pattern in the same low frequency channel for figure 3(b). Instead, we observe some horizontal and vertical line patterns clearly in the middle frequency region. The simple experiment implies that the low frequency region of textures may not necessarily contain significant information.

Thus, an appropriate way to perform the wavelet transform for textures is to detect the significant frequency channels and then to decompose them further. The above idea leads naturally to a new type wavelet transform called the tree-structured wavelet transform. Note that it is usually unnecessary to decompose all subimages in each scale to achieve a full decomposition. To avoid a full decomposition, we use a maximum criterion of textural measures to locate dominant information in each frequency channels and to decide whether a decomposition is needed for a particular output. With this transform, we are able to zoom into any desired frequency channels for further decomposition.

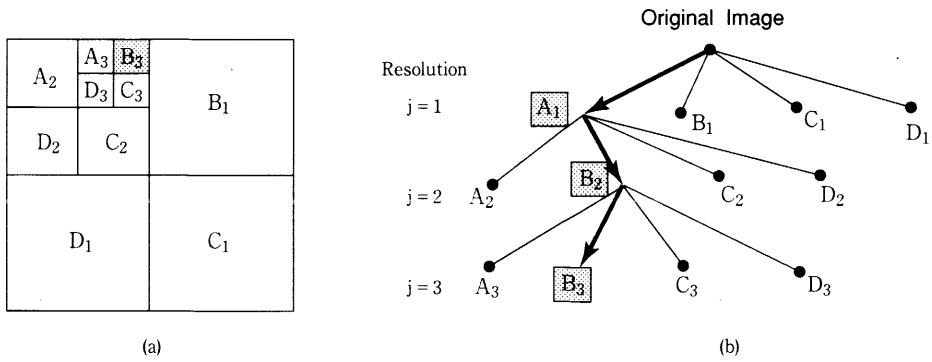

Figure 4 (a) Channel decomposition. (b) Quadtree representation.

The example is shown in figure 4(a). The decomposition is no longer simply applied to the low frequency channels recursively. Instead, it can be applied to any other frequency channels. The quadtree structure with respect to each tree-structured wavelet transform is illustrated in figure 4(b).

Mallat's experiment [8] suggests that by using wavelet decomposition, statistics based on first-order distribution of gray levels might be sufficient for preattentive perception of textural difference. Hence, we define the feature as the criterion for locating dominant information in each subimage is the average of energy distribution. If the subimage is x(m,n), with $1 \leq m \leq M$ and $1 \leq n \leq N$, the feature can be written in mathematical equation as follows,

$$e = \frac{1}{MN} \sum_{m=1}^{M} \sum_{n=1}^{N} | x(m,n) | \tag{7}$$

This parameter is also known as averaged l_1-norm for the energy function. This feature is chosen due to its simplicity to locate dominant frequency channels.

3. Fuzzy C-Means Clustering

Clustering or unsupervised classification is defined as finding "natural" grouping in a set of measurement where a certain measurement vector represents properties or attributes of some underlying set of classes. The data from a multichannel image tend to cluster within the corresponding class in a feature-space diagram. The objective of this cluster analysis is to divide a given data set into subsets or clusters. In general, the clustering has to verify the following two constraints: there is no empty cluster, every sample must be classified. The number of clusters, c, is generally known, otherwise it can be determined a posteriori by an examination of cluster coherence against supervised information. In hard c-partition, a sample belongs to one and only one cluster, with no distinction between samples close to their cluster center and mixed samples (near the cluster border). On the contrary, fuzzy-c-partition methods, which are based on a notion of similarity (called membership) between samples and

clusters, can deal with mixed samples. The membership values calculated using the fuzzy c-means algorithm will all be real numbers between 0 and 1. The closer the value comes to 1, the higher is the membership of the object.

In this paper, we employ the fuzzy c-means method in a multiresolution system that uses no training. The other clustering methods have been proposed in the past, for example, we can use a Kohonen's self-organization feature mapping method [7]. It is superior to the fuzzy c-means method from the two viewpoints of simplicity and computational time of the algorithm, unless we set a large size of neural network. However, it is not easy to define the number of neurons in a competitive layer, so that we must do it by trial and error. Moreover, it is difficult to classify the resembled pattern since the number of neurons is fixed. These two points are disadvantages when we use the Kohonen's self-organization method. On the other hand, using the fuzzy c-means method, we can classify the input data based on Euclidean distance between them, and in addition, since it is not necessary to fix the number of output categories, we can classify them based on a threshold value of Euclidean distance. We limit ourselves to the use of the Euclidean norm, because other norms such as the diagonal norm, or the Mahalonobis norm, imply heavy calculations. An illustration of the image segmentation with fuzzy c-means method is shown in figure 5.

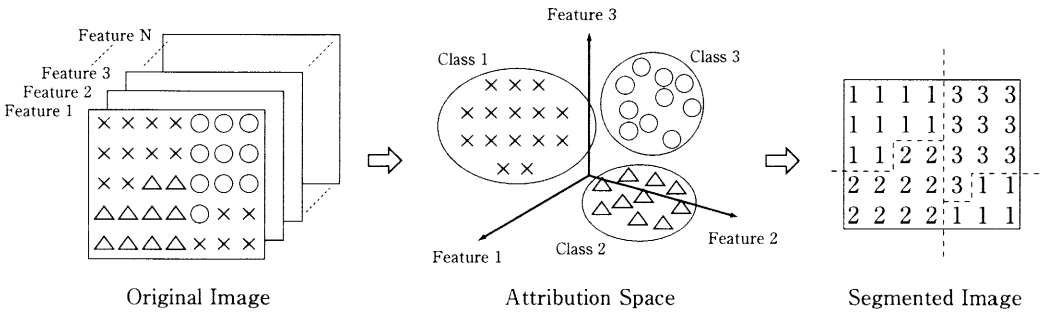

Figure 5. Image segmentation with fuzzy c-means method.

The algorithm of fuzzy c-means method is described as follows. We consider the input pattern as N-dimensional vectors. At first, we pick up C cluster centers $\vec{v}_i$, i=1 ... C. We consider them as the initial classes. The Euclidean distance d($\vec{x}_j$, $\vec{v}_i$) between pixels $\vec{x}_j$, and cluster centers $\vec{v}_i$, is computed by

$$d\left(\vec{x}_j, \vec{v}_i\right) = \sqrt{(x_{j1}-v_{i1})^2+(x_{j2}-v_{i2})^2+\cdots+(x_{jN}-v_{iN})^2} \tag{8}$$

Next, we calculate the membership μ_{ij} for each pixel using equations as follows:

$$g_{ij} = \frac{1}{d^2\left(\vec{x}_j, \vec{v}_i\right)} \tag{9}$$

$$G_j = \sum_{i=1}^{K} g_{ij} \tag{10}$$

$$\mu_{ij} = \begin{cases} g_{ij} / G_j & \text{if } \vec{x}_j \notin \vec{v}_i \\ 1 & \text{if } \vec{x}_j \in \vec{v}_i \end{cases} \tag{11}$$

After that, we recomputed the estimates for new cluster centers $\vec{v}_i$.

$$v_i = \frac{\sum_{j=1}^{M} \mu_{ij}^2 \vec{x}_j}{\sum_{j=1}^{M} \mu_{ij}^2} \tag{12}$$

Repeat these processes until the $\vec{v}_i$ are consistent. After clustering them, we output a resulting image colored as the representation of each class.

Bastin [3] shows that the use of fuzzy c-means method has been found useful for identifying land-cover-classes application and gave the best result compared with linear mixture modeling and maximum likelihood classification.

4. Image-Segmentation Procedure Using Multiresolution Analysis

Image-segmentation procedure using multiresolution analysis, as shown schematically in figure 6, consists of two steps: feature extraction and clustering process.

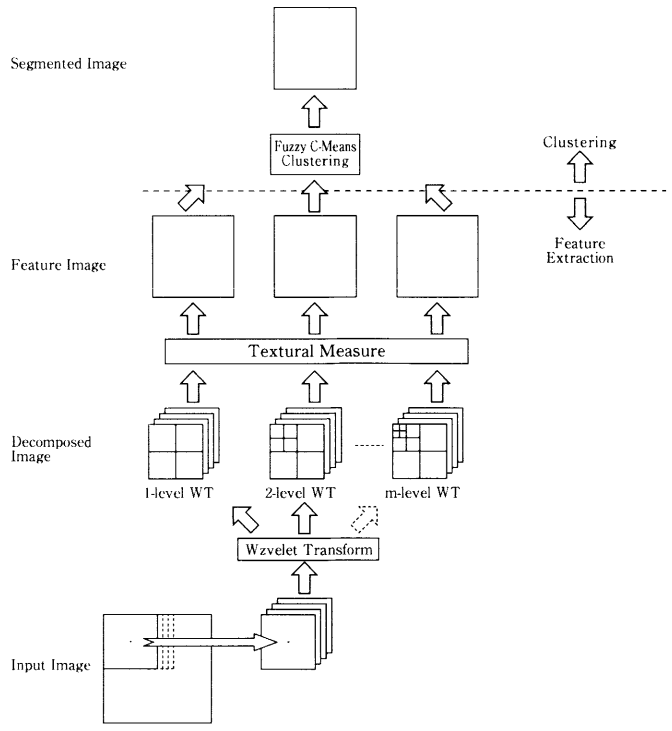

Figure 6. Block diagram of image-segmentation procedure using multiresolution analysis.

First, we extract a window-size image from the input image. During the first phase, an extracted window-size image is decomposed into four subimages using a bank of filters (see table 1). Afterwards, we apply a statistical parameter as the textural measure to each subimage (decomposed image). If the textural measure of a subimage is greater than others, we continue the decomposition in this region since it contains more information. Repeat the decomposition until the minimal size of the subimage has exceeded. From our experience, the size of the smallest subimages should not be less than 8 × 8 pixels. It is because if they have a very narrow size, the location and the feature value may vary widely so that the feature may not be robust. Next, we move the window image one pixel, and perform the decomposition process again. Repeat these steps continuously to cover the whole image. This phase results in a set of feature images that contains a set of feature vectors. These feature vectors that correspond to different resolution of decomposed image are assumed to capture and characterize different scales of textures from the input image effectively. In the second phase, all the input pixels of the feature images are classified based on their associated vector values by using fuzzy c-means clustering algorithm. This second phase will result in a segmented image.

The main advantage of the present method is that these computations can be performed in a lower-dimensional space that essentially preserves the discriminative information and provides features that are approximately decorrelated. In the implementation, there will be only one feature component for each resolution of the image. This will reduce substantially the amount of computation and simplify the segmentation process, while not seriously affecting the overall performance.

5. Experiments and Discussion

A test image 256 × 256 pixels in size, which is generated by combining four Brodatz-like microtextures is illustrated in figure 7. The four textures had their histograms equalized to abolish variation in illumination. Flat histograms ensured that there were no intertexture differences in luminance distributions. Therefore these four textures are indistinguishable on the basis of first-order statistics.

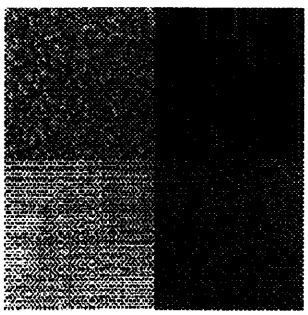

Figure 7. A test image consist of four Brodatz-like microtextures

The size selection of the moving window depends on the size of the repetitive structure in the textural region. The smaller window size will make the textural feature not robust, while the greater window size will lead to a higher computational cost. Empirically, the use of 32 × 32 pixels moving window-size gives a very satisfactory result. Consequently, a 2-level tree-structured wavelet transform is appropriate.

The decomposition is implemented using the 16-tap Daubechies wavelet basis. We have, however, performed the same experiments with other orthogonal wavelet filters, namely Haar, 4-tap Daubechies, and Battle Lemarie filters. In all experiments, the results give nearly similar performance. In other words, the results are largely independent of the choice of filter banks.

From the experiment, the average of the energy distribution feature as the textural measure gives the maximum value always on the low frequency channel. This is because the feature measure textural uniformity that usually located in the low frequency. In addition, the 16-tap wavelet filter has high regularity property, which causes most of the important structural information in the image to be projected into the low frequency subimages. The feature images with a depth of two are shown in figure 8. The finer resolution components at scale j=1 is illustrated in figure 8(a), while figure 8(b) represent the coarser information at scale j=2.

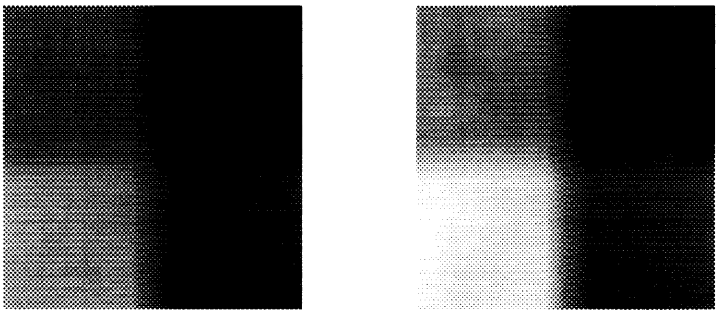

Figure 8. (a) Feature image at finer resolution j=1. (b) Feature image at coarser resolution j=2.

Figure 9 shows the final result of the segmentation process into four classes. The segmentation process is visually satisfying as is evident from the single cluster representations. All textures have been correctly identified. Note that the result has been obtained without prior knowledge of the spatial relationship of different sites. The small incorrectness is shown at the joint border of different textures. This is mainly caused by the consequence of the shifting window. When it reaches to the middle of different textures, the energy features calculated are taken from more than one texture. Consequently, the result will correspond to the texture which have the nearest features.

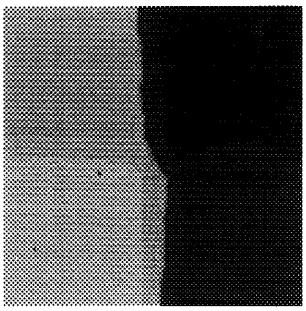

Figure 9. Four cluster segmented image.

The approach is also applicable for remote-sensing images. In such case, many satellite-images contain texture-like structures. In this study, we use a SPOT satellite image 256 × 256 pixels in size of Tangerang region including Cengkareng International Airport, Indonesia. The image as shown in figure 9(a), has 10-m spatial resolution.

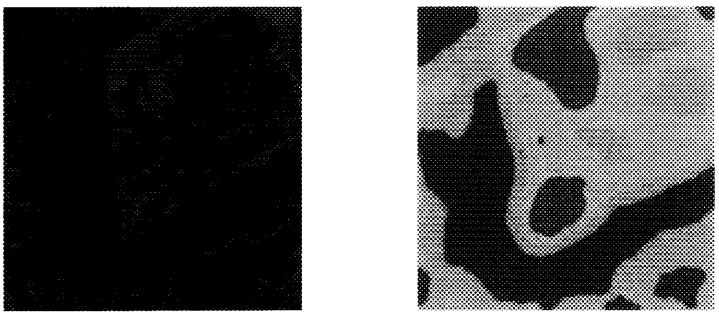

(a) (b)

Figure 9. (a) Original image. (b) Four cluster segmented image.

The result of segmentation process into four classes is illustrated in figure 9(b). The achieved segmentation is visually satisfying. It is seen that the process can discriminate the regions that have different texture characteristics. Vegetation, residential area as well as some objects in the airport are well separated. Moreover, some buildings in the airport are detected. Note that the segmentation was obtained without a postprocessing step. From this result it is concluded that this procedure can give a reasonable result.

In these two examples, the uses of fuzzy and hard c-means method give very little variation in performance. The reason is that the feature vectors extracted from both images contain very few mixed samples.

These experiments have been conducted using a personal computer PC/Pentium 300 MHz. All of the computations involving multiresolution wavelet transform, textural measure as well as fuzzy c-means clustering are implemented in Visual Basic language. Computing the feature vector of an extracted window-size image takes only 0.07 seconds of CPU time. This

quick response is mainly due to the property of wavelet decomposition that has fast algorithm, which is based on convolutions with a bank of filters. Beside that, wavelet decomposition use only 2MN dynamic memory units for an image of size MN. Therefore this procedure is suitable for the use of larger size of image. In some cases, it may be reasonable to replace the computation of the previous textural feature extraction methods that derived from fourier spectrum [1], gray level cooccurrence matrix [2], local statistics [14], in order to benefit by a better compromise between texture measurement accuracy, computation time and computer storage.

6. Conclusion

A procedure to segment an image based on textural features has been presented. To demonstrate the capability of the procedure, we have implemented it in the artificial and real world images. The experimental results indicated that the procedure could give a reasonable result, while improving the time computation performance.

The main conclusions that can be drawn from the present analysis and from our segmentation experiments are as follows:

1. The multiresolution approach lends itself quite well to texture segmentation. In all cases, a multiscale feature extraction with two or three levels led to better results than a single resolution analysis.
2. The multiresolution properties of the wavelet transform are beneficial for texture discrimination. The wavelet transform has many properties (multiresolution representation, orthogonality, fast algorithms, etc.) that are relevant to this type of application.
3. By using wavelet decomposition, the feature derived from statistics based on first-order distribution of gray levels in the subimages is sufficient for preattentive perception of textural difference.
4. Experiments with different wavelet transforms indicate very little variation in performance with respect to the choice of filters.
5. Finally, the main advantage of this new procedure is to provide adequate segmentation at a much lower cost.

References:

[1] M.F.Augusteijn, L.E.Clemens, and K.A.Shaw, "Performance Evaluation of Texture Measures for Ground Cover Identifikcation in Satellite Images by Means of a Neural Network Classifier," *IEEE Trans. on Geoscience and Remote Sensing*, vol.33, no.3, pp.616-625, May 1995.

[2] A.Baraldi and F.Parmiggiani, "An Investigation of the Textural Characteristics Associated with Gray Level Cooccurance Matrix Statistical Parameters," *IEEE Trans. on Geoscience and Remote Sensing*, vol.33, no.2, pp.293-304, Mar.1995.

[3] L.Bastin, "Comparison of Fuzzy C-Means Classification, Linear Mixture Modelling and MLC Probabilities as Tools for Unmixing Coarse Pixels," *Int. J. Remote Sensing*, vol.18, no.17, pp.3629-3648, Nov.1997.

[4] C.Bouman and B.Liu, "Multiple Resolution Segmentation of Textured Images," *IEEE Trans. on Pattern Analysis and Machine Intelligence*, vol.13, no.2, pp.99-113, Feb.1991.

[5] R.L.Cannon, J.V.Dave, and J.C.Bezdek, "Efficient Implementation of the Fuzzy C-Means Clustering Algorithms," *IEEE Trans. on Pattern Analysis and Machine Intelligence*, vol.PAMI 8, no.2, pp.248-255, Mar.1986.

[6] D.Dunn, W.E.Higgin, and J.Wakeley, "Texture Segmentation Using 2-D Gabor Elementary Functions," *IEEE Trans. on Pattern Analysis and Machine Intelligence*, vol.16, no.2, pp.130-149, Feb.1994.

[7] Y.Ito and S.Omatu, "Category Classification Method Using a Self-Organizing Neural Network," *Int. J. Remote Sensing*, vol.18, no.4, pp.829-845, Mar.1997

[8] S.G.Mallat, "A Theory for Multiresolution Signal Decomposition: The Wavelet Representation," *IEEE Trans. on Pattern Analysis and Machine Intelligence*, vol.11, no.7, pp.674-693, July 1989.

[9] S.Mallat and S.Zhong, "Characterization of Signals from Multiscale Edges," *IEEE Trans. on Pattern Analysis and Machine Intelligence*, vol.14, no.7, pp.710-732, July 1992.

[10] B.S.Manjunath and R.Chellapa, "Unsupervised Texture Segmentation Using Markov Random Field Models," *IEEE Trans. on Pattern Analysis and Machine Intelligence*, vol.13, no.5, pp.478-482, May 1991.

[11] B.S.Manjunath and W.Y.Ma, "Texture Features for Browsing and Retrieval of Image Data," *IEEE Trans. on Pattern Analysis and Machine Intelligence*, vol.18, no.8, pp.837-842, Aug.1996.

[12] N.R.Pal and J.C.Bezdek, "Cluster Validity for the Fuzzy C-Means Model," *IEEE Trans. on Fuzzy Systems*, vol.3, no.3, pp.370-379, Aug.1995.

[13] R.Schalkoff, *Pattern Recognition: Statistical, Structural and Neural Approaches*. NY: John Wiley & Sons, Inc., 1992.

[14] A.H.S.Solberg and A.K.Jain, "Texture Fusion and Feature Selection Applied to SAR Imagery," *IEEE Trans. on Geoscience and Remote Sensing*, vol.35, no.2, pp.475-479, Mar.1997.

[15] K.L.Vincken, A.S.E.Koster, and M.A.Viergever, "Probabilistic Multiscale Image Segmentation," *IEEE Trans. on Pattern Analysis and Machine Intelligence*, vol.19, no.2, pp.109-120, Feb.1997.